Journal of Alloys and Compounds 489 (2010) 353–356

Contents lists available at ScienceDirect

Journal of Alloys and Compounds

journal homepage: www.elsevier.com/locate/jallcom

Thermoelectric properties of molybdenum oxides $LnMo_8O_{14}$ (Ln = La, Ce, Pr, Nd and Sm)

Jianxiao Xu[a,*], Monica Sonne[a], Nini Pryds[a], Holger Kleinke[b,*]

[a] *Fuel Cells and Solid State Chemistry Division, Risø National Laboratory for Sustainable Energy, Technical University of Denmark, 4000 Roskilde, Denmark*
[b] *Department of Chemistry, University of Waterloo, Waterloo, Ontario, Canada N2L 3G1*

ARTICLE INFO

Article history:
Received 17 August 2009
Received in revised form 31 August 2009
Accepted 31 August 2009
Available online 30 September 2009

Keywords:
Thermoelectrics
Semiconductors
Molybdenum oxides
Clusters
Electronic structures

ABSTRACT

The series $LnMo_8O_{14}$ (Ln = La, Ce, Pr, Nd and Sm) containing bicapped Mo_8 clusters was synthesized via solid state reaction at 1673 K. Oxides of this type were reported to be narrow gap semiconductors. Our Seebeck coefficient measurements show that some of these reduced molybdenum oxides exhibit a thermopower of above −100 μV/K at room temperature, which is promising for the thermoelectric application. The highest power factor of 71 μW/mK^2 was obtained for $SmMo_8O_{14}$ at 1152 K.

1. Introduction

Thermoelectric (TE) energy conversion can be used to generate electricity from temperature gradients. Hence power can be harvested from waste heat using TE materials, e.g. from the exhaust in automotives [1]. Because of the increasing demand and limited availability of energy sources, there is strong and renewed interest in advancing thermoelectric materials. Past research shows that the best TE materials are narrow band gap semiconductors composed of heavy elements [2–5], exhibiting a large Seebeck coefficient, S, combined with high electrical conductivity, σ, and low total thermal conductivity, κ, in order to achieve a high figure of merit, $ZT = S^2\sigma T/\kappa$ (T is the absolute temperature).

Because of their good thermal stability at high temperatures in air, oxides are promising candidates for recovering waste heat. However, oxides had not been considered as suitable materials for thermoelectrics until 1997, when Terasaki et al. [6] discovered that a single crystal of cobalt oxide $NaCo_2O_4$ exhibited excellent thermoelectric performances. After that, p-type layered cobalt oxides were of great interest, and several new candidate materials, including $Ca_3Co_4O_9$ [7,8] were developed through extensive studies. In recent years, some n-type thermoelectric oxides with the perovskite-type structure were studied, e.g. $SrTiO_3$ [9–13] and $CaMnO_3$ [14,15]. However, compared with p-type cobalt oxides, n-type thermoelectric oxides are still much less efficient. For the fabrication of thermoelectric modules, both high-performance p-type and n-type thermoelectric oxides are required, so it is crucial to find new n-type thermoelectric oxides with higher ZT values.

Molybdenum oxides, such as $LaMo_8O_{14}$ [16,17], $LaMo_5O_8$ [18,19], $Y_4Mo_4O_{11}$ [20], $Pr_4Mo_9O_{18}$ [21] and $La_5Mo_{32}O_{54}$ [22] containing different Mo clusters with strong metal–metal bonds between the Mo atoms, are usually semiconductors with narrow band gaps, which could be potential materials for thermoelectric applications. In this work, we will introduce a series of new n-type oxides ($LnMo_8O_{14}$, Ln = La, Ce, Pr, Nd and Sm) containing Mo_8 clusters showing promising thermoelectric properties.

2. Experimental

Five phase-pure $LnMo_8O_{14}$ (Ln = La, Ce, Pr, Nd and Sm) were prepared from stoichiometric mixtures of Ln_2O_3 (except Pr_6O_{11} for $PrMo_8O_{14}$), Mo and MoO_3, by solid state reaction. The purity of all starting materials was above 99%. The starting materials were thoroughly mixed, and cold-pressed into pellets by a uniaxial pressing tool. After that, the pellets were loaded into a furnace and heated up to 1673 K for 24 h under an argon flow. All final products turned out to be black powders and were examined by powder X-ray diffraction (Bruker D8) at room temperature. No secondary phases were detected in the X-ray powder patterns, indicating pure phases.

3. Electronic structure calculation

The LMTO method (LMTO = linear muffin tin orbitals) [23] was utilized for the electronic structure calculations. This method is based on the density functional theory (DFT) [24,25], which pos-

---

* Corresponding authors.
E-mail addresses: jiax@risoe.dtu.dk (J. Xu), kleinke@uwaterloo.ca (H. Kleinke).

0925-8388/$ – see front matter © 2009 Elsevier B.V. All rights reserved.
doi:10.1016/j.jallcom.2009.09.136

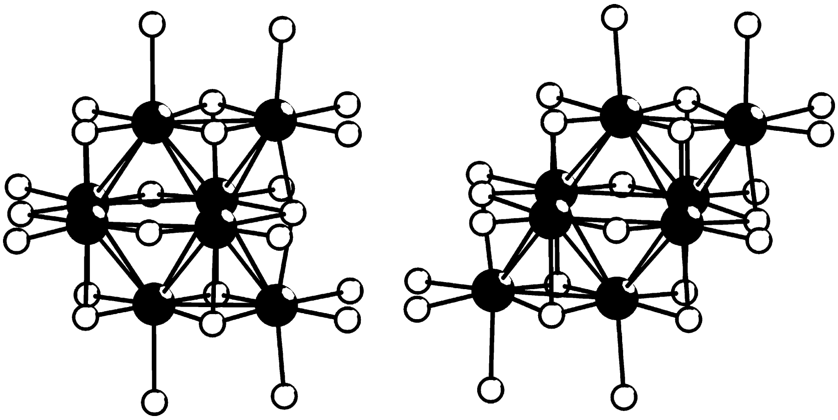

Fig. 1. Two different bicapped Mo_8 clusters: *cis* (left) and *trans* (right). Mo: black; O: white.

tulates that the total energy is a unique function of the electron density and has its minimum at the ground state density. The LMTO method uses the atomic spheres approximation (ASA) [26], and the local density approximation (LDA) [27] for the exchange and correlation energies in the DFT. Sufficient independent k points of the first Brillouin zone were chosen via an improved tetrahedron method [28].

4. Physical property measurements

At first, Spark Plasma Sintering (SPS) method was attempted to obtain high dense pellets for measurements. The powdered materials were loaded into a graphite die with the diameter of 12.7 mm, and sintering was carried out by placing the materials under a uniaxial pressure of 110 MPa, then heating under vacuum to 1573 K. However, these molybdenum oxides start to decompose before they can be densified during this process. Finally we pressed the ground phase-pure sample of these oxides into pellets by a uniaxial press followed by a cold-isostatic press. The pellets were then densified by sintering in a high temperature furnace at 1473 K for 5 h under argon for physical property measurements. The densities for all pellets were calculated to be around 65% of the theoretical values after measuring volume and weight.

Thermoelectric properties such as electrical conductivity (σ) and Seebeck coefficient (S) of the five compounds were measured from room temperature to 1152 K under vacuum on bar shaped pellets with approximate dimensions of 3 mm × 3 mm × 8 mm using the ZEM3-M10 unit from ULVAC Technologies, Inc. Japan.

5. Results and discussion

5.1. Crystal structure

Molybdenum oxides with the formula $LnMo_8O_{14}$ (Ln = La, Ce, Pr, Nd and Sm) [16,17,29–32] were reported to contain Mo_8 clusters. $LaMo_8O_{14}$ and $CeMo_8O_{14}$ crystallize in the orthorhombic crystal system with the space group *Pbcn* as determined by the single crystal X-ray diffraction, although there is another different modification obtained from fused-salt electrolysis for $LaMo_8O_{14}$ [16]. The crystal structure contains two different bicapped Mo_8 clusters with a 1:1 ratio. According to the different face capping, the Mo_8 clusters were defined differently as *cis* and *trans* as shown in Fig. 1. Each Mo atom is connected to 5 O atoms, and the two symmetry-independent La^{3+} or Ce^{3+} cations are surrounded by 12 O atoms forming a distorted cuboctahedron. The Pr compound contains two different types of Mo_8 clusters with the ratio of 2:1 for *cis* and *trans*, therefore resulting in a different space group, namely *Pbca*. On the other hand, the Nd and Sm compounds crystallize in the space group of *Aba*2 composed exclusively of *cis*-bicapped Mo_8 clusters.

According to Mahan [33], ZT increases with an increasing B parameter, which increases with the increase of the number of degenerate bands (N_V), mobility (μ), and effective mass (m^*), while it is inversely proportional to the lattice thermal conductivity:

$$B \propto \frac{N_V \mu (m^*)^{3/2}}{\kappa_{ph}}$$

In order to achieve high ZT values, high mobility, thus covalent bonds within the structure, and low lattice thermal conductivity, thus heavy elements in the compound, are favorable. The reason why oxides were not considered as suitable for thermoelectric application for a long time was due to their low mobility and molecular masses. Strong Mo–Mo bonds with an average distance of 2.7 Å within the Mo_8 clusters for the present studied oxides are beneficial for high mobility. Moreover, the presence of heavy lanthanide elements and molybdenum in these oxides is advantageous for achieving low lattice thermal conductivity.

5.2. Electronic structure

The electronic structure of $LaMo_8O_{14}$ was calculated as an example, in order to extract information for predicting and explaining transport properties. The densities of states (DOS) for this compound have been described elsewhere [34], so only the band structure results will be discussed here. Since all atomic sites in the structure of $LaMo_8O_{14}$ are fully occupied, the model of this

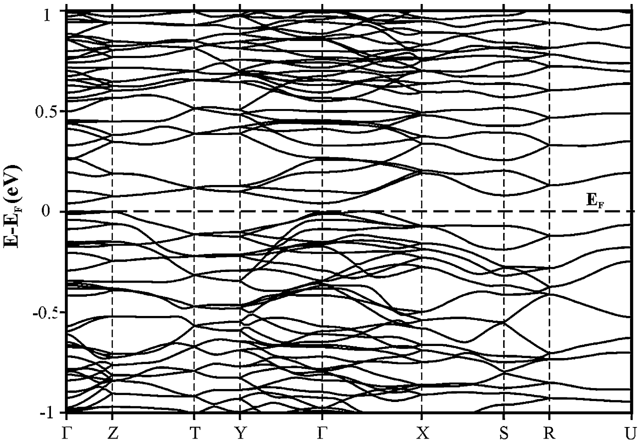

Fig. 2. Electronic band structure of $LaMo_8O_{14}$.

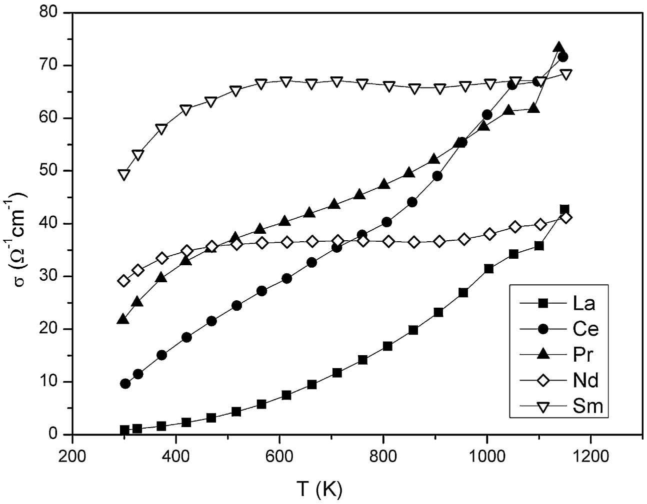

Fig. 3. Electrical conductivity measurements of LnMo$_8$O$_{14}$.

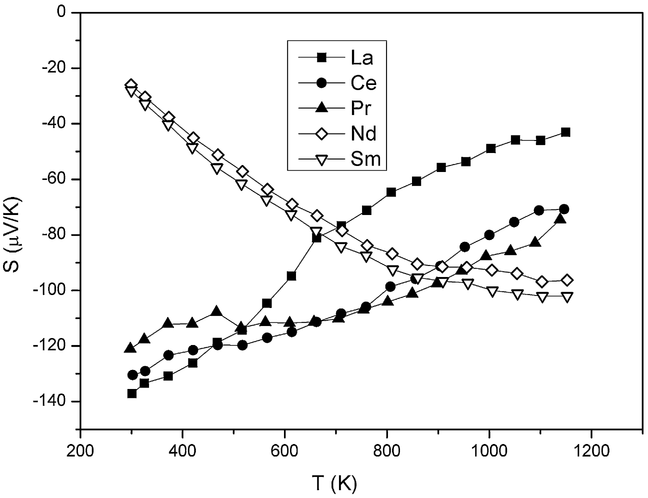

Fig. 4. Seebeck coefficient measurements of LnMo$_8$O$_{14}$.

compound chosen for the calculation was taken directly from the single crystal structure determination [17] with the *Pbcn* symmetry. The calculated electronic band structures of LaMo$_8$O$_{14}$ are shown in Fig. 2. The bands in the vicinity of the Fermi level, E_F, arbitrarily placed at 0 eV, are rather flat, indicative of a high effective mass (m^*), which will lead to a high Seebeck coefficient.

Our band structure calculation indicates that LaMo$_8$O$_{14}$ is a semiconductor with a direct band gap of 0.05 eV at the Γ point, which is quite comparable to the result of Gautier et al. [34]. Later, semiconducting behavior was confirmed by the electrical conductivity measurement.

5.3. Physical properties

The electrical and magnetic properties of LnMo$_8$O$_{14}$ (Ln = La, Ce, Pr, Nd and Sm) single crystals have been previously measured below room temperature [34,35]. In this article, thermoelectric properties of these molybdenum oxides obtained from bulk materials will be discussed. Typical for semiconductors, the electrical conductivity increases with the increasing temperature. The electrical conductivity measurements shown in Fig. 3 indicate that the five compounds are semiconductors from room temperature up to 1152 K in accord with the prediction from the electronic structure calculation. The electrical conductivity at room temperature was determined to be 1.0 Ω^{-1} cm^{-1} for LaMo$_8$O$_{14}$, 9.6 Ω^{-1} cm^{-1} for CeMo$_8$O$_{14}$, 21.7 Ω^{-1} cm^{-1} for PrMo$_8$O$_{14}$, 29.2 Ω^{-1} cm^{-1} for NdMo$_8$O$_{14}$, and 49.5 Ω^{-1} cm^{-1} for SmMo$_8$O$_{14}$. These values are significantly lower than the reported ones measured on single crystals, e.g. 25 Ω^{-1} cm^{-1} for LaMo$_8$O$_{14}$, and 200 Ω^{-1} cm^{-1} for PrMo$_8$O$_{14}$. This is probably due to the large number of boundaries between grains compared to single crystals, i.e. the lower density of the measured samples leads to a lower conductivity [36]. With the increase of temperature, the conductivity of NdMo$_8$O$_{14}$ and SmMo$_8$O$_{14}$ increases slower than for LaMo$_8$O$_{14}$, CeMo$_8$O$_{14}$, and PrMo$_8$O$_{14}$. In fact, the former two reach a plateau around 500 K, while the other's conductivity increases throughout the whole temperature range (Fig. 3).

Seebeck coefficient measurements (Fig. 4) show that the dominant charge carriers in all five oxides are n-type. LaMo$_8$O$_{14}$ exhibits the highest Seebeck coefficient of −137 μV/K at room temperature, which is comparable with other outstanding thermoelectric oxides like NaCo$_2$O$_4$ [6], SrTi$_{1-x}$Ta$_x$O$_3$ [13], and CaMn$_{1-x}$Nb$_x$O$_3$ [15]. As for LaMo$_8$O$_{14}$, CeMo$_8$O$_{14}$, and PrMo$_8$O$_{14}$, the absolute value of the Seebeck coefficient decreases with increasing temperature, which is not favorable for thermoelectric applications at high temperatures. The maximum is expected to occur below room temperature, in accord with the calculated small band gap [33]. NdMo$_8$O$_{14}$ and SmMo$_8$O$_{14}$, on the other hand, exhibit lower Seebeck coefficient values of −26 and −28 μV/K at room temperature, respectively. With the increase of temperature, NdMo$_8$O$_{14}$ and SmMo$_8$O$_{14}$ show a different trend than the other three compounds, which is probably a consequence of the different structure of the Nd and Sm compounds, possibly due to the absence of *trans*-Mo$_8$ clusters. Since the absolute values of the Seebeck coefficient of these two oxides increase with increasing temperature, the change in carrier concentration is less pronounced, which agrees with the plateau in the conductivity curves.

Using the electrical conductivity and Seebeck coefficient data, the power factor ($S^2\sigma$) values of these five compounds were evaluated as shown in Fig. 5. The power factor of LaMo$_8$O$_{14}$, CeMo$_8$O$_{14}$, and PrMo$_8$O$_{14}$ increases with increasing temperature, and reaches a maximum at an intermediate temperature (ca. 800 K). On the other hand, the power factor of the NdMo$_8$O$_{14}$ and SmMo$_8$O$_{14}$ compounds was found to increase continuously with the increase of temperature. The maximum value of the power factor is 71 μW/mK^2 at 1152 K for SmMo$_8$O$_{14}$, which is much lower than that of the state-of-art high temperature thermoelec-

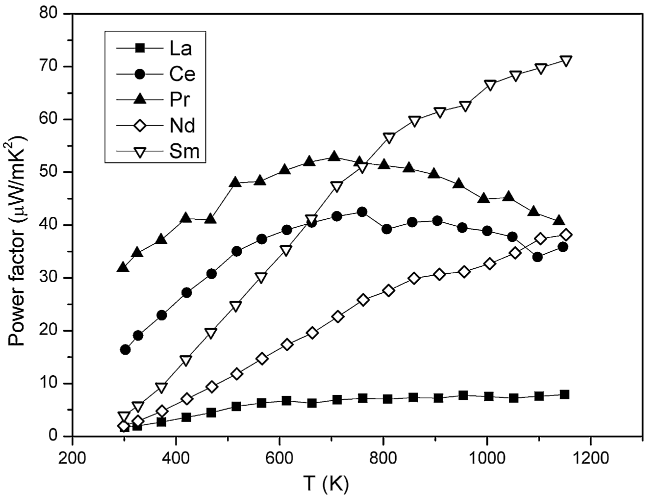

Fig. 5. The power factor of LnMo$_8$O$_{14}$.

tric materials [37], such as skutterudites [38], $Yb_{14}MnSb_{11}$ [39], and $Ni_xMo_3Sb_{5.4}Te_{1.6}$ [40].

6. Conclusion

Five molybdenum oxides, $LaMo_8O_{14}$, $CeMo_8O_{14}$, $PrMo_8O_{14}$, $NdMo_8O_{14}$, and $SmMo_8O_{14}$ were synthesized via high temperature solid state reactions. The electronic structure of $LaMo_8O_{14}$ was investigated. The electrical conductivity and Seebeck coefficients of all these five oxides were measured from room temperature to 1152 K, and all five oxides are dominated by n-type charge carriers. $NdMo_8O_{14}$ and $SmMo_8O_{14}$, composed of different arrangements of Mo_8 clusters, possess different transport properties. $LaMo_8O_{14}$ shows a high Seebeck coefficient at room temperature and $SmMo_8O_{14}$ exhibits the highest power factor among these five compounds, which is still too low for thermoelectric applications. Further optimization, e.g. material densification and proper doping, will be attempted to improve the thermoelectric properties.

Acknowledgements

The work was initialized at the University of Waterloo in Canada supported by the Natural Sciences and Engineering Research Council of Canada, and finalized in the Fuel Cells and Solid State Chemistry Division at Risø National Laboratory in Denmark. Consolidation attempts via spark plasma sintering by T. Holgate and Dr. T.M. Tritt from Clemson University, and Dr. M. Nygren from Stockholm University, are acknowledged.

References

[1] J. Yang, T. Caillat, Mater. Res. Bull. 31 (2006) 224–229.
[2] T.M. Tritt, Science 272 (1995) 1276–1277.
[3] D.M. Rowe, CRC Handbook of Thermoelectrics, CRC Press, Boca Raton, FL, 1995.
[4] T.M. Tritt, Science 283 (1999) 804–805.
[5] F.J. DiSalvo, Science 285 (1999) 703–706.
[6] I. Terasaki, Y. Sasago, K. Uchinokura, Phys. Rev. B 56 (1997) 12685–12687.
[7] R. Funahashi, I. Matsubara, H. Ikuta, T. Takeuchi, U. Mizutani, S. Sodeoka, Jpn. J. Appl. Phys. 39 (2000) 1127–1129.
[8] A.C. Masset, C. Michel, A. Maignan, O. Toulenonde, F. Studer, B. Raveau, J. Hejtmanek, Phys. Rev. B 62 (2000) 166–175.
[9] T. Okuda, K. Nakanishi, S. Miyasaka, Y. Tokura, Phys. Rev. B 63 (2001) 113104/1–1113104/4.
[10] H. Muta, K. Kurosaki, S. Yamanaka, J. Alloys Compd. 350 (2003) 292–295.
[11] S. Ohta, T. Nomura, H. Ohta, K. Koumoto, J. Appl. Phys. 97 (2005) 034106/1–134106/4.
[12] S. Ohta, T. Nomura, H. Ohta, M. Hirano, H. Hosono, K. Koumoto, Appl. Phys. Lett. 87 (2005) 092108/1–192108/3.
[13] Y. Cui, J.R. Salvador, J. Yang, H. Wang, G. Amow, H. Kleinke, J. Electron. Mater. 38 (2009) 1002–1007.
[14] G. Xu, R. Funahashi, Q. Pu, B. Liu, R. Tao, G. Wang, Z. Ding, Solid State Ionics 171 (2004) 147–151.
[15] L. Bocher, M.H. Aguirre, D. Logvinovich, A. Shkabko, R. Robert, M. Trottmann, A. Weidenkaff, Inorg. Chem. 47 (2008) 8077–8085.
[16] H. Leligny, P. Labbe, M. Ledesert, M. Hervieu, B. Raveau, W.H. McCarroll, Acta Crystallogr. B 49 (1993) 444–454.
[17] G. Kerihuel, J. Tortelier, P. Gougeon, Acta Crystallogr. C 52 (1996) 2389–2393.
[18] H.-J. Koo, M.-H. Whangbo, W.H. McCarroll, M. Greenblatt, R. Gautier, J.-F. Halet, P. Gougeon, Solid State Commun. 108 (1998) 539–544.
[19] P. Gougeon, P. Gall, J.-F. Halet, R. Gautier, Acta Crystallogr. B 59 (2003) 472–478.
[20] P. Gall, N. Barrier, R. Gautier, P. Gougeon, Inorg. Chem. 41 (2002) 2879–2885.
[21] J. Tortelier, P. Gougeon, Inorg. Chem. 37 (1998) 6229–6236.
[22] J. Tortelier, P. Gall, H. Noel, P. Gougeon, J. Solid State Chem. 152 (2000) 403–411.
[23] H.L. Skriver, The LMTO Method, Springer, Berlin, Germany, 1984.
[24] P. Hohenberg, W. Kohn, Phys. Rev. B 136 (1964) 864–871.
[25] R.G. Parr, W. Yang, Density-functional Theory of Atoms and Molecules, Clarendon Press, Oxford, UK, 1989.
[26] O.K. Andersen, Phys. Rev. B 12 (1975) 3060–3083.
[27] L. Hedin, B.I. Lundqvist, J. Phys. C 4 (1971) 2064–2083.
[28] P.E. Blöchl, O. Jepsen, O.K. Andersen, Phys. Rev. B 49 (1994) 16223–16233.
[29] G. Kerihuel, P. Gougeon, Acta Crystallogr. C 51 (1995) 787–790.
[30] G. Kerihuel, P. Gougeon, Acta Crystallogr. C 51 (1995) 1475–1478.
[31] P. Gougeon, R.E. McCarley, Acta Crystallogr. C 47 (1991) 241–244.
[32] J. Tortelier, P. Gougeon, Acta Crystallogr. C 53 (1997) 668–671.
[33] G.D. Mahan, J. Appl. Phys. 65 (1989) 1578–1583.
[34] R. Gautier, O.K. Andersen, P. Gougeon, J.-F. Halet, E. Ganadell, J.D. Martin, Inorg. Chem. 41 (2002) 4689–4699.
[35] K.V. Ramanujachary, E.B. Jones, M. Greenblatt, W.H. McCarroll, J. Solid State Chem. 117 (1995) 261–268.
[36] N. Soheilnia, H. Xu, H. Zhang, T.M. Tritt, I. Swainson, H. Kleinke, Chem. Mater. 19 (2007) 4063–4068.
[37] H. Kleinke, Chem. Mater. (2010), doi:10.1021/cm901591d.
[38] G.S. Nolas, D.T. Morelli, T.M. Tritt, Annu. Rev. Mater. Sci. 29 (1999) 89–116.
[39] S.R. Brown, S.M. Kauzlarich, F. Gascoin, G.J. Snyder, Chem. Mater. 18 (2006) 1873–1877.
[40] H. Xu, K.M. Kleinke, T. Holgate, H. Zhang, Z. Su, T.M. Tritt, H. Kleinke, J. Appl. Phys. 105 (2009) 053703/1–053703/5.